

Threshold switching and memory behaviors of epitaxially regrown GaN-on-GaN vertical p - n diodes with high temperature stability

Kai Fu, Houqiang Fu, *Student Member, IEEE*, Xuanqi Huang, Tsung-Han Yang, Hong Chen, Izak Baranowski, Jossue Montes, Chen Yang, Jingan Zhou and Yuji Zhao, *Member, IEEE*

Abstract—This letter reports the observation of threshold switching and memory behaviors of epitaxially regrown GaN-on-GaN vertical p - n diodes. This mechanism was ascribed to the conductive path formed by traps in the insulating layer at the regrowth interface after soft breakdown. The device can reliably switch more than 1000 cycles at both room temperature and 300 °C with small fluctuation on the set and reset voltage. The set voltage increased with the increasing temperature due to the enhanced thermal detrapping effect that made it harder to form conductive path at high temperatures. Besides, the device showed memory behaviors when the reset voltage was higher than 4.4 V. This work can serve as important references to further developing GaN-based memory devices and integrated circuits.

Index Terms—Gallium nitride, wide bandgap semiconductor, p - n diodes, breakdown, threshold switching, memory.

I. INTRODUCTION

RESISTIVE random access memory (RRAM) has garnered considerable research interests and shown promising performance such as excellent scalability, low programming voltage, and fast write/read speed [1], [2]. For the standalone and large capacity nonvolatile memory (NVM), the cross-point (or crossbar) array is an attractive architecture for the RRAM. To cut off the sneak path current of the unselected cells for a large-scale cross-point array, either RRAMs with self-rectification characteristics can be used [3], [4], or a selector device (with asymmetry or nonlinearity) can be connected in series with the RRAM cell at each cross-point [2], [5]-[7]. Many threshold switching selector devices have been proposed, such as p - n diodes [8], bidirectional varistors [9], mixed-ion-electronic-conduction (MIEC) [10], [11], Ovonic threshold switching (OTS) [12], [13], metal-insulator transition (MIT) [14], and programmable metallization cell (PMC) [2]. The threshold and resistive switching have been observed in a

This work is supported by ARPA-E PNDIODES Program monitored by Dr. Isik Kizilyalli (grant number DE-AR0000868) and partially supported by NASA HOTTech Program grant number 80NSSC17K0768. Access to the NanoFab was supported, in part, by NSF contract ECCS-1542160.

Kai Fu, Houqiang Fu, Xuanqi Huang, Tsung-Han Yang, Hong Chen, Izak Baranowski, Jossue Montes, Chen Yang, Jingan Zhou and Yuji Zhao are with the School of Electrical, Computer, and Energy Engineering, Arizona State University, Tempe, AZ, 85287 USA (e-mail: kaifu@asu.edu; yuji.zhao@asu.edu).

wide variety of material systems, such as NiO, TiO_x, CuO_x, ZrO_x, ZnO_x, HfO_x, TaO_x, AlO_x, TiN/HfO₂, p-CuO/n-InZnO, Ni/TiO₂/Ni, Pt/VO₂/Pt, TiN/NbO₂/W, Ag/a-Si, and W/Cu_xS/W [1], [2], [15]-[18]. However, no reliable switching behaviors have been observed in these memristors above 200 °C, limiting their potential applications in harsh electronics. Although one type of robust memristor has recently proposed based on 2D materials (graphene/MoS_{2-x}O_x/graphene) with an operating temperature up to 340 °C [19], mass production and electrical stability are still challenging for the 2D materials. III-nitrides were also used to fabricate the resistive switching devices, such as Al-rich AlN films based on the forming and breaking tunneling paths by charging and discharging in the Al nanoparticles [20], and AlN/n-GaN based on forming/rupturing electron transport channel by trapping/detrapping electrons due to traps resulted from nitrogen vacancies of AlN [21]. As one of the most promising candidates for applications in power electronic systems, GaN power devices can realize remarkable improvements in energy conversion efficiency, switching frequency, and system volume, due to its wide bandgap properties [22], [23]. The GaN-based memory devices are desirable to integrate with the mature nitride high electron mobility transistors (HEMTs) and facilitate a new generation GaN based integrated circuits [21], [24]. However, no GaN based threshold switching and memory behaviors at high temperatures above 200 °C have been reported.

In this work, we demonstrated threshold switching and memory behaviors in the epitaxially regrown GaN-on-GaN vertical p - n diodes, which have not been reported before, to the best of our knowledge. The device showed reproducible

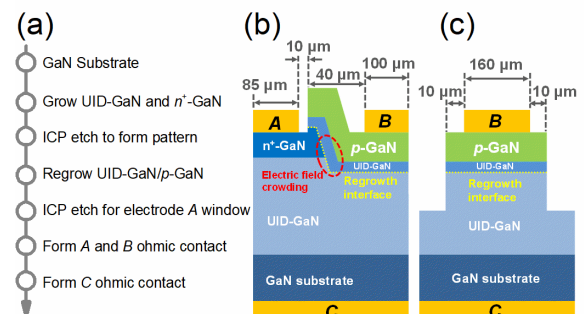


Fig. 1. (a) Process flow of the device growth and fabrication. Cross-sectional view of (b) device A and (c) device B.

switching behaviors with good endurance performance of 1000 cycles test at both room temperature and 300 °C. The set voltage increased with temperature and remained stable from 200 °C to 300 °C.

II. GROWTH AND DEVICE FABRICATION

The samples were homoepitaxially grown by metalorganic chemical vapor deposition (MOCVD) on *c*-plane *n*-GaN substrates with a carrier concentration of $\sim 10^{18} \text{ cm}^{-3}$ from Sumitomo Electric Industries Ltd.. The growth temperature was $\sim 1040 \text{ }^\circ\text{C}$ and hydrogen (H_2) was used as the carrier gas. Trimethylgallium (TMGa), ammonia (NH_3), silane (SiH_4) and bis(cyclopentadienyl)magnesium (Cp_2Mg) were used as the precursors for Ga, N, Si dopants, and Mg dopants, respectively. We propose a trench-type *p-n* diode structure, with regrowth interface next to the trench corner, that reveals the memory effect. Figure 1(a) shows the growth and process flow. As shown in Fig. 1(b), $7 \text{ }\mu\text{m}$ unintentionally doped (UID) GaN ($1 \times 10^{16} \text{ cm}^{-3}$) and $1 \text{ }\mu\text{m}$ *n*⁺-GaN ($1 \times 10^{18} \text{ cm}^{-3}$) were first grown on the GaN substrate. Then $1.5 \text{ }\mu\text{m}$ GaN was etched away to form regrowth patterns by inductively coupled plasma (ICP), followed by 300 nm UID-GaN and $1 \text{ }\mu\text{m}$ *p*-GaN ($3 \times 10^{17} \text{ cm}^{-3}$) successively regrown on the etched surface. The regrown layers on *n*⁺-GaN were selectively etched by ICP to form ohmic contact area for electrode A. Deep ICP etching was carried out to form mesa isolation for the devices. Electrodes A and B were formed by electron-beam evaporation using metal stacks of Ti/Al/Ni/Au (20/130/50/150 nm) and Pd/Ni/Au (10/20/30 nm), respectively. Finally, the Ti/Al/Ni/Au metal stacks were also deposited on the backside of the GaN substrate to form ohmic contacts for electrode C. Devices without the trench structure but with regrowth interface were also fabricated on the sample wafer for reference [device B in Fig. 1(c)]. The dimensions of the devices are shown in Fig. 1. Current-voltage (*I-V*) characteristics were measured using a Keithley 2400 sourcemeter. The compliance current was set to be 100 mA in this work. The duration for which the device stays at a certain voltage was 100 ms. The voltage steps for reverse and forward biases were 0.5 V and 0.2 V, respectively.

III. RESULTS AND DISCUSSIONS

As shown in Fig. 2, forward characteristics of the *p-n* diodes (*B-A* for the lateral, *B-C* for the vertical) before soft breakdown (SB) were first measured, as shown by blue lines in Fig. 2(b) and (c). Then, reverse characteristics were measured to initiate the SB as shown by the blue and green lines in Fig. 2(a). Then, reverse and forward characteristics of the diodes after SB were measured as shown by red lines in Fig. 2. The vertical *p-n* junction in device A was found showing stable and significant hysteresis, or threshold switching behavior, at the forward bias as shown in Fig. 2(c). The numbers in Fig. 2(c) shows the voltage sweep direction from “1” to “6” in a cycle. The threshold switching process includes a high resistance state (HRS) and a low resistance state (LRS). As usually defined in literatures, the switching event from HRS to LRS is called “set” process, the switching event from LRS to HRS is called the

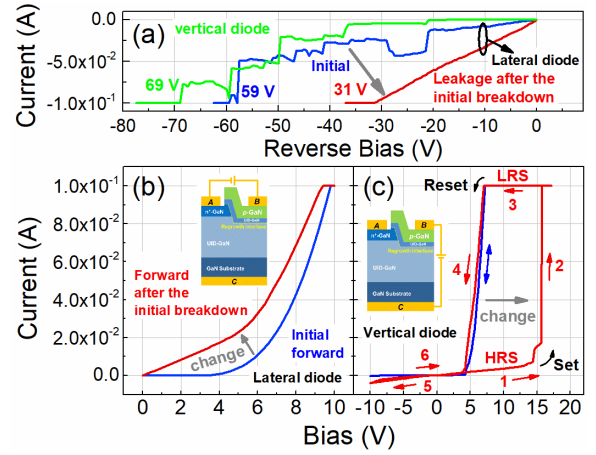


Fig. 2. (a) Reverse *I-V* curves of the lateral diode in device A before and after the SB. (b) Forward *I-V* curves of the lateral diode before and after the SB. (c) *I-V* curves of the vertical diode before and after the SB. Numbers and arrows indicate the sequence of voltage sweeping.

“reset” process. The set voltage ($\sim 15 \text{ V}$) is defined as the voltage at which the current reaches the compliance current and the reset voltage ($\sim 3.6 \text{ V}$) is the back-sweep voltage at which the current drops to 1 mA in this work. The threshold switching behavior at reverse bias region (even to -40 V) was not noticeably observed compared with the forward one. In this work, the reverse SB served as the forming process. Since this is a *p-n* diode, the emission and disappearance of blue light from the *p-n* junction was another indicator of the switching process. The threshold switching behavior was only observed in vertical diodes. It was found that the SB of either the lateral or vertical *p-n* junction in device A could be used as the forming process, whereas the SB of the lateral *p-n* junction was a more effective way that almost all the vertical diodes in device A showed threshold switching behavior. The higher efficiency may be attributed to electric crowding effect at the trench corner [25], as indicated in Fig. 1(b). The electric crowding at the lateral interface may avoid the hard breakdown of the horizontal regrowth interface in the forming process. The detailed study on the physical mechanism is an ongoing research topic. Furthermore, the device B with a simpler structure (only horizontal regrowth interface) also showed the threshold switching behavior while it was not observed in conventional as-grown vertical GaN *p-n* diodes. These indicate that the regrowth interface is the necessary condition for the threshold switching behavior. Besides, the device can reliably switch more than 1000 cycles at room temperature with very

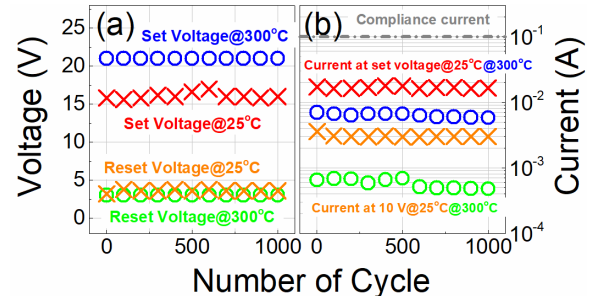


Fig. 3. Cycling demonstration of the vertical diode in device A on (a) set voltage and (b) current at HRS.

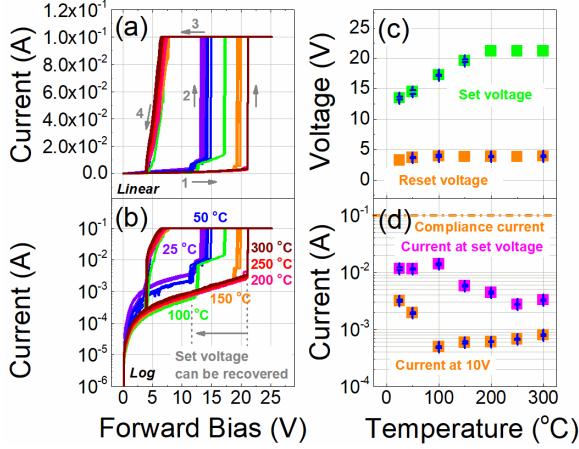


Fig. 4. Forward I - V characteristics of the vertical diode in device A at different temperatures in (a) linear scale and (b) semi-log scale. (c) Set voltage and (d) current at HRS at different temperatures. Five sweeping cycles are shown at each temperature.

small fluctuation on the set voltage and the current at HRS, as depicted in Fig. 3. The current at the set voltage means the current at the HRS state right before the sudden increase of current. This retention analysis was measured by direct voltage scanning mode [5].

After the 1000 cycles of endurance test on the device, we carried out the high temperature test. Figure 4(a) and 4(b) shows the I - V characteristics by linear scale and semi-log scale, respectively. As shown in Fig. 4(c), the set voltage increased with increasing temperature and became stable (21.2 V) above 200 °C. Figure 4(d) shows the current at HRS decreased with increasing temperature. In addition, the high temperature performance is reversible: all the device parameters will recover to the initial values when the temperature decreases to the room temperature. The 1000 cycles of endurance test at 300 °C shown in Fig. 3(a) also confirmed the high temperature stability of the switching behavior.

Figure 5(a) presents the I - V curve in log-log scale. The LRS curve follows the p - n diode characteristics. The HRS I - V curve can be explained by the trap-assisted space charge limited current (SCLC) theory (the Ohmic region I - V , and the Child's square law region I - V^2 followed by a steep increase in current) [1], [20]. It is postulated that after the SB, the regrowth interfacial layer [26] may possess properties similar to a thin insulating layer with a large amount of trap states which leads to the HRS. The traps form/rupture conductive path by

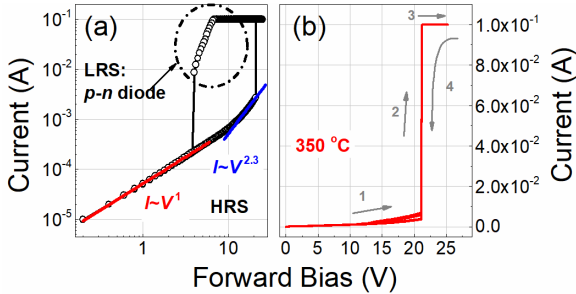


Fig. 5. (a) Log-log scale I - V curves of different temperatures with linear fitting at different voltage regions. (b) I - V curves of the vertical diodes at 350 °C with 5 sweeping cycles.

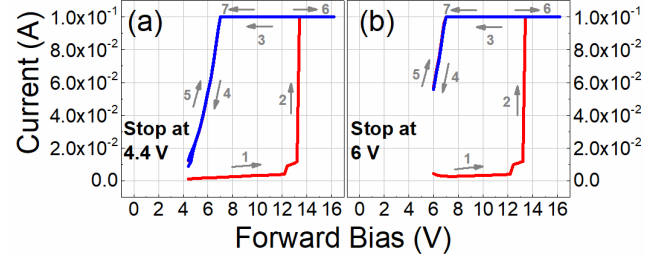


Fig. 6. I - V curves of vertical diode in device A with different sweeping voltages starting from (a) 4.4 V and (b) 6 V. Numbers indicate the sweeping direction and five sweeping cycles are shown for each condition.

trapping/detrapping carriers. Similar mechanisms have already been reported [21], [24]. When the voltage increases from 0 V to above the set voltage, the insulating layer (HRS) becomes conductive by trapping carriers. Then the device behaves as a conventional p - n diode (LRS) when the voltage decreases to reset voltage that is a little higher than the turn-on voltage. When the voltage continues to decrease to lower voltages, the insulating layer becomes insulating again by detrapping carriers because the p - n diode is turned off and few carriers can be trapped to form the conductive path. The set voltage shifts to higher values with increased temperature due to the enhanced detrapping effect at high temperatures. When the temperature exceeds 350 °C, the conductive path forms and maintains only when the applied bias is higher than the set voltage, as shown in Fig. 5(b). However, the aforementioned reset process recovered (shown in Fig. 4) when the temperature decreased.

We also found that the traps-based conductive path could be maintained when the start/stop sweeping voltage was a little higher than the turn-on voltage of the GaN p - n diode. This memory behavior, characterized by varying the sweeping stop voltage at 4.4 V and 6 V are shown in Fig. 6(a) and 6(b), respectively. The device performance would transfer from HRS to LRS when the forward bias was higher than the set voltage. When the stop voltage was higher than 4.4 V, the device performance would stay at LRS, otherwise the device would go back to HRS.

IV. CONCLUSION

The epitaxially regrown GaN-on-GaN vertical p - n diodes showed threshold switching and memory behaviors after SB of the regrowth interface. The threshold switching behaviors are repeatable and stable at high temperatures up to 300 °C. Further work should be carried out to adjust the set voltage and to decrease the HRS current.

ACKNOWLEDGMENT

We acknowledge the use of facilities within the Eyring Materials Center at Arizona State University. The device fabrication was performed at the Center for Solid State Electronics Research at Arizona State University.

REFERENCES

- [1] S. Yu, "Resistive Random Access Memory (RRAM): From Devices to Array Architectures," in *Synthesis Lectures on Emerging Engineering Technologies*. vol. 2, Morgan & Claypool, 2016, pp. 1-79, doi: 10.2200/S00681ED1V01Y201510EET006

- [2] J. Yoo, J. Woo, J. Song, and H. Hwang, "Threshold switching behavior of Ag-Si based selector device and hydrogen doping effect on its characteristics," *AIP Adv.*, vol. 5, pp. 127221-1-127221-6, Dec. 2015, doi: 10.1063/1.4938548.
- [3] X. A. Tran, B. Gao, J. F. Kang, X. Wu, L. Wu, Z. Fang, Z.R. Wang, K.L. Pey, Y.C. Yeo, A.Y. Du, M. Liu, B.Y. Nguyen, M.F. Li, and H.Y. Yu, "Self-rectifying and forming-free unipolar HfOx based-high performance RRAM built by fab-availalbe materials," in *2011 IEEE International Electron Devices Meeting (IEDM)*, pp. 31.2.1-31.2.4, Dec. 2011, doi: 10.1109/IEDM.2011.6131648
- [4] K.-H. Kim, S. H. Jo, S. Gaba, and W. Lu, "Nanoscale resistive memory with intrinsic diode characteristics and long endurance," *Appl. Phys. Lett.*, vol. 96, pp. 053106-1-053106-3, Feb. 2010, doi: 10.1063/1.3294625.
- [5] K. Lee, J. W. Park, Y. Tchoe, J. Yoon, K. Chung, H. Yoon, S. Lee, C. Yoon, B. H. Park, and G. C. Yi, "Flexible resistive random access memory devices by using NiOx/GaN microdisk arrays fabricated on graphene films," *Nanotechnology*, vol. 28, May 19. 2017, doi: 10.1088/1361-6528/aa6763.
- [6] A. Chen, "Memory selector devices and crossbar array design: a modeling-based assessment," *J. Comput. Electron.*, vol. 16, pp. 1186-1200, Sept. 2017, doi: 10.1007/s10825-017-1059-7.
- [7] S. Jeonghwan, W. Jiyong, A. Prakash, L. Daeseok, and H. Hyunsang, "Threshold Selector With High Selectivity and Steep Slope for Cross-Point Memory Array," *IEEE Electron Device Lett.*, vol. 36, pp. 681-683, May 2015, doi: 10.1109/LED.2015.2430332.
- [8] M.-J. Lee, Y. Park, B.-S. Kang, S.-E. Ahn, C. Lee, K. Kim, W. Xianyu, G. Stefanovich, J.-H. Lee, S.-J. Chung, Y.-H. Kim, C.-S. Lee, J.-B. Park, I.-G. Baek, and I.-K. Yoo, "2-stack 1D-1R Cross-point Structure with Oxide Diodes as Switch Elements for High Density Resistance RAM Applications," in *2007 IEEE International Electron Devices Meeting (IEDM)*, Washington, DC, USA, 2007, pp. 771-774, doi: 10.1109/IEDM.2007.4419061.
- [9] W. Lee, J. Park, J. Shin, J. Woo, S. Kim, G. Choi, S. Jung, S. Park, D. Lee, E. Cha, H. D. Lee, S. G. Kim, S. Chung, and H. Hwang, "Varistor-type bidirectional switch ($J_{MAX} > 10^7 A/cm^2$, selectivity $\sim 10^4$) for 3D bipolar resistive memory arrays" in *2012 Symposium on VLSI Technology (VLSIT)*, Honolulu, HI, USA, 2012, pp. 37-38, doi: 10.1109/VLSIT.2012.6242449.
- [10] K. Gopalakrishnan, R. S. Shenoy, C. T. Rettner, K. Virwani, D. S. Bethune, R. M. Shelby, G. W. Burr, A. Kellock, R. S. King, K. Nguyen, A. N. Bowers, M. Jurich, B. Jackson, A. M. Friz, T. Topuria, P. M. Rice, and B. N. Kurdi, "Highly-scalable novel access device based on Mixed Ionic Electronic conduction (MIEC) materials for high density phase change memory (PCM) arrays," in *2010 Symposium on VLSI Technology (VLSIT)*, Honolulu, Hawaii, USA, 2010, pp. 205-206, doi: 10.1109/VLSIT.2010.5556229.
- [11] K. Virwani, G. W. Burr, R. S. Shenoy, C. T. Rettner, A. Padilla, T. Topuria, P. M. Rice, G. Ho, R. S. King, K. Nguyen, A. N. Bowers, M. Jurich, M. Brightsky, E.A. Joseph, A. J. Kellock, N. Arellano, B. N. Kurdi and K. Gopalakrishnan, "Sub-30nm scaling and high-speed operation of fully-confined Access-Devices for 3D crosspoint memory based on mixed-ionic-electronic-conduction (MIEC) materials," in *2012 IEEE International Electron Devices Meeting (IEDM)*, San Francisco, CA, USA, 2012, pp. 2.7.1-2.7.4, doi: 10.1109/IEDM.2012.6478967.
- [12] Y. Koo, S. Lee, S. Park, M. Yang, and H. Hwang, "Simple Binary Ovonic Threshold Switching Material SiTe and Its Excellent Selector Performance for High-Density Memory Array Application," *IEEE Electron Device Lett.*, vol. 38, pp. 568-571, May 2017, doi: 10.1109/LED.2017.2685435.
- [13] W. Czubatjy and S. J. Hudgens, "Invited paper: Thin-film Ovonic threshold switch: Its operation and application in modern integrated circuits," *Electronic Mater. Lett.*, vol. 8, pp. 157-167, Apr. 2012, doi: 10.1007/s13391-012-2040-z.
- [14] E. Cha, J. Park, J. Woo, D. Lee, A. Prakash, and H. Hwang, "Comprehensive scaling study of NbO2 insulator-metal-transition selector for cross point array application," *Appl. Phys. Lett.*, vol. 108, pp. 153502-1-153502-3, Apr. 2016, doi: 10.1063/1.4945367.
- [15] S. Lim, J. Yoo, J. Song, J. Woo, J. Park, and H. Hwang, "Excellent threshold switching device ($I_{off} \sim 1$ pA) with atom-scale metal filament for steep slope (< 5 mV/dec), ultra low voltage ($V_{dd} = 0.25$ V) FET applications," in *2016 IEEE International Electron Devices Meeting (IEDM)*, San Francisco, CA, USA, 2016, pp. 34.7.1-37.7.4, doi: 10.1109/IEDM.2016.7838543.
- [16] R. Aluguri and T. Tseng, "Overview of Selector Devices for 3-D Stackable Cross Point RRAM Arrays," *IEEE J. Electron Devices Soc.*, vol. 4, pp. 294-306, Sept. 2016, doi: 10.1109/JEDS.2016.2594190.
- [17] D.-H. Kwon, K. M. Kim, J. H. Jang, J. M. Jeon, M. H. Lee, G. H. Kim, X.-S. Li, G.-S. Park, B. Lee, S. Han, M. Kim, and C. S. Hwang, "Atomic structure of conducting nanofilaments in TiO2 resistive switching memory," *Nat. Nanotechnol.*, vol. 5, pp. 148-53, Feb. 2010, doi: 10.1038/nnano.2009.456.
- [18] P. Calka, E. Martinez, V. Delaye, D. Lafond, G. Audoit, D. Mariolle, N. Chevalier, H. Grampeix, C. Cagli, V. Jousseau and C. Guedj, "Chemical and structural properties of conducting nanofilaments in TiN/HfO2-based resistive switching structures," *Nanotechnology*, vol. 24, no. 8, pp. 085706 (1-9), Feb. 2013, doi:10.1088/0957-4484/24/8/085706.
- [19] M. Wang, S. H. Cai, C. Pan, C. Y. Wang, X. J. Lian, Y. Zhuo, K. Xu, T. J. Cao, X. Q. Pan, B. G. Wang, S. J. Liang, J. J. Yang, P. Wang, and F. Miao, "Robust memristors based on layered two-dimensional materials," *Nat. Electron.*, vol. 1, pp. 130-136, Feb. 2018, doi: 10.1038/s41928-018-0021-4.
- [20] Y. Liu, T. P. Chen, P. Zhao, S. Zhang, S. Fung, and Y. Q. Fu, "Memory effect of Al-rich AlN films synthesized with rf magnetron sputtering," *Appl. Phys. Lett.*, vol. 87, pp. 033112-1-033112-3, Jul. 2005, doi: 10.1063/1.2000337.
- [21] Y. Chen, H. Song, H. Jiang, Z. Li, Z. Zhang, X. Sun, D. Li, and G. Miao, "Reproducible bipolar resistive switching in entire nitride AlN/n-GaN metal-insulator-semiconductor device and its mechanism," *Appl. Phys. Lett.*, vol. 105, pp. 193502-1-193502-5, Nov. 2014, doi: 10.1063/1.4901747.
- [22] T. J. Flack, B. N. Pushpakaran, and S. B. Bayne, "GaN Technology for Power Electronic Applications: A Review," *J. Electron. Mater.*, vol. 45, pp. 2673-2682, Jun. 2016, doi: 10.1007/s11664-016-4435-3.
- [23] X. C. Huang, Z. Y. Liu, Q. Li, and F. C. Lee, "Evaluation and Application of 600 V GaN HEMT in Cascade Structure," *IEEE T. Power Electr.*, vol. 29, pp. 2453-2461, May. 2014, doi: 10.1109/Tpel.2013.2276127.
- [24] Y. R. Chen, Z. M. Li, Z. W. Zhang, L. Q. Hu, H. Jiang, G. Q. Miao, and H. Song, "Annealing effect on the bipolar resistive switching characteristics of a Ti/Si₃N₄/n-GaN MIS device," *J. Alloys Compd.*, vol. 740, pp. 816-822, Jan. 2018, doi: 10.1016/j.jallcom.2018.01.072.
- [25] Y. H. Zhang, M. Sun, Z. H. Liu, D. Piedra, J. Hu, X. Gao, and T. Palacios, "Trench formation and corner rounding in vertical GaN power devices," *Appl. Phys. Lett.*, vol. 110, May 8. 2017, doi: 10.1063/1.4983558.
- [26] K. Fu, H. Fu, H. Liu, S. R. Alugubelli, T.-H. Yang, X. Huang, H. Chen, I. Baranowski, J. Montes, F. A. Ponce, and Y. Zhao, "Investigation of GaN-on-GaN vertical p-n diode with regrown p-GaN by metalorganic chemical vapor deposition," *Appl. Phys. Lett.*, vol. 113, pp. 233502, Dec. 3. 2018, doi: 10.1063/1.5052479.